



ELSEVIER

Available online at www.sciencedirect.com

ScienceDirect

journal homepage: www.elsevier.com/locate/he

Steam reforming of shale gas in a packed bed reactor with and without chemical looping using nickel based oxygen carrier

Zainab Ibrahim S G Adiya*, Valerie Dupont, Tariq Mahmud

School of Chemical and Process Engineering (SCAPE), The University of Leeds, Leeds LS2 9JT, UK

ARTICLE INFO

Article history:

Received 30 July 2017

Received in revised form

10 February 2018

Accepted 12 February 2018

Available online xxx

Keywords:

Shale gas

Steam reforming

Chemical looping

Hydrogen

NiO catalyst

Nickel oxygen carrier

ABSTRACT

The catalytic steam reforming of shale gas was examined over NiO on Al₂O₃ and NiO on CaO/Al₂O₃ in the double role of catalysts and oxygen carrier (OC) when operating in chemical looping in a packed bed reactor at 1 bar pressure and S:C 3. The effects of gas hourly space velocity GHSV (h⁻¹), reforming temperatures (600–750 °C) and catalyst type on conventional steam reforming (C-SR) was first evaluated. The feasibility of chemical looping steam reforming (CL-SR) of shale gas at 750 °C with NiO on CaO/Al₂O₃ was then assessed and demonstrated a significant deterioration after about 9 successive reduction-oxidation cycles. But, fuel conversion was high over 80% approximately prior to deterioration of the catalyst/OC, that can be strongly attributed to the high operating temperature in favour of the steam reforming process.

© 2018 The Authors. Published by Elsevier Ltd on behalf of Hydrogen Energy Publications LLC. This is an open access article under the CC BY license (<http://creativecommons.org/licenses/by/4.0/>).

Introduction

Conventional steam reforming (C-SR) has been the leading technology for H₂ production [1–3] for the past 70 years [4]. C-SR consists as a minimum of two basic steps of steam reforming (SR) and water gas shift (WGS), followed by a final separation stage. In the endothermic reforming stage, syngas, a mixture of CO, CO₂, H₂O, H₂, is generated at temperature between 800 and 950 °C and medium pressure of around 20–35 atm, usually in the presence of a nickel oxide catalyst, activated to Ni by chemical reduction in a one-off pre-treatment [5,6], by reacting high-temperature steam and hydrocarbon volatile or gaseous feedstock (usually methane or natural gas, but also naphtha). WGS, which reacts the CO in the syngas with steam to produce additional H₂ with CO₂ as

co-product is mildly exothermic, and thus is operated separately at a lower temperature between 200 and 400 °C [7–9] though does not achieve full conversion due to a strong equilibrium effect. The total energy demand of the process is overall endothermic, necessitating an external source of energy [10]; normally the unreacted fraction of fuel caused by the high pressure in the reformers is burned in a furnace which houses the reformer reactors to provide the energy, and top-up from the fuel feedstock might even be necessary to meet the reformers' heat demand. The separation process marks the final stage of the process. Unreacted CH₄, CO, H₂O, and product CO₂ from the syngas leaving the WGS reactor is separated from the H₂ at this stage. A number techniques are available and can be used to perform the separation process, most commonly pressure swing absorption (PSA), but also membranes, cryogenics [11,12] are the most commonly used

* Corresponding author.

E-mail address: xeadiya@yahoo.com (Z.I. S G Adiya).

<https://doi.org/10.1016/j.ijhydene.2018.02.083>

0360-3199/© 2018 The Authors. Published by Elsevier Ltd on behalf of Hydrogen Energy Publications LLC. This is an open access article under the CC BY license (<http://creativecommons.org/licenses/by/4.0/>).

separation techniques. Chemical absorption for example CO₂ scrubbing using methyldiethanolamine (MDEA), activated methyldiethanolamine (aMDEA) are also used for separation but purity of H₂ is less than with PSA, membrane or cryogenics [13]. Detailed overview on membrane separation and chemical absorption can be found in Adhikari and Fernando [14] and Yildirim et al. [13] respectively.

Despite having reached technological maturity, steam reforming is one of the most energy consuming processes in hydrocarbon processing and ammonia production via its heating requirement, with other drawbacks such as emission of greenhouse gases and other air pollutants and high operational and maintenance costs [10,15,16]. Globally, researchers are focusing on finding alternative energy efficient technologies that can mitigate the economic and environmental impacts of the forecasted large increases in hydrogen demand [17]. One of such alternative is the chemical looping steam reforming (CL-SR) technology. The latter combines chemical looping combustion (CLC) and steam reforming to minimise the energy expenditure from the C-SR process. A metal oxide is used as an intermediate to transport oxygen from air to fuel in order to provide heat of oxidation to the endothermic H₂ production process. If a suitable metal oxide is used as the oxygen carrier, the CLC system on its own can be operated in such a way that the exhaust gas consists of CO₂ and H₂O only, and allows for subsequent water condensation, compression and storage of CO₂, evading the costly gas separation steps [18,19] of post combustion capture. When combined with steam reforming, the OC can be chosen for its catalytic activity in the steam reforming reactions (SR and WGS), thus allowing the production of a reformat undiluted with N₂ despite having used air as the oxidant, drastically reducing the demand in external heating and separation burdens. Therefore, CLC is one of the most energy efficient approaches to carbon capture from power production or fuel upgrading [20,21].

The large scale application of CLC and CL-SR is still dependent upon the obtainability of suitable OC(s). A suitable OC should have some certain basic characteristics such ability to undergo multiple reduction and oxidation cycles, high mechanical strength and oxygen transport capacity and should be eco-friendly [17,22]. Various metal oxides such as Fe₃O₄/Fe₂O₃, MnFe₂O₄(Jacobsite), MnFe₂O₄ (Iwakiite), NiO, CuO, MnO₂, CeO₂, Co₃O₄ and perovskite-type oxides including their blends have been tested as OC in either gaseous or solid fuels [23,24]. However, nickel-based oxides have been proved as one of the most promising and utilised OC in CL-SR processes because of their high reactivity and selectivity, negligible volatility and thermal steadiness which are favourable factors for elevated temperature and high gas turbine CLC [17,24]. Nickel-based oxides are also regarded as first good choice for hydrogen production [22].

As first step in the packed bed configuration, the CL-SR process gas is fed into the reactor loaded with catalytically active OC where both reduction of oxygen carrier (OC) also termed oxygen transfer material (OTM) in the literature- and steam reforming occur semi-simultaneously, generating H₂ rich syngas. A fraction of the feedstock is expected to be used as reductant in the metal oxide reduction to produce H₂O and CO₂ but the remainder would then reform to pure CO₂ and H₂

[25] by the catalytically active reduced metal. The second step involves oxidation of the OC back to its initial state under air feed, producing a separate N₂ effluent. Thus, the major differences between the C-SR process and CL-SR process is the reduction of the OC/catalyst by the hydrocarbon feedstock and the oxidation reaction that marks the end of each cycle. Due to H₂ and CO or CO₂ being the desired products of CL-SR as opposed to heat, this requires keeping the air to fuel ratio low to avoid the fuel from been oxidised completely to H₂O and CO₂ [26]. A detailed description of CL-SR with a schematic illustrating the potential benefits of the process compared to the conventional C-SR process when using unconventional gas as feedstock can be found in our previous study [17] and Luo et al. [24].

Diverse feedstocks such as liquids by-products of biomass [27], natural gas, naphtha and coal are presently utilised and studied for the steam reforming process. However, 90% of the H₂ produced globally originates from steam reforming of fossil fuels [28–30]; with natural gas dominating the net H₂ production [31,32]. This is not surprising owing to the favourable hydrogen-to-carbon ratio of natural gas. In addition, the new found abundance of unconventional natural gas that is readily available and can be supplied at a viable cost, showed natural gas will continue to be a very important energy mix [33,34]. The vast quantity of the gas that was earlier inaccessible worldwide reserves is presently accessible with the newly developed technologies as well [34–36]. The present boom in shale gas (a form of natural gas found trapped within shale formation) production [37] in the world also foresees that gas will remain the main feedstock of steam reforming in near term [17]. However, all of the studies on C-SR and CL-SR processes focussed pure methane as fuel [38–43], for CL-SR process low steam to carbon ratios were focused on [44–46] and additionally most of the previous studies such as [45,47–49] used fluidised bed reactor (Air and fuel reactor separate) for the CL-SR process.

In the present study, a detailed experimental analysis of H₂ production from shale gas containing C₂ and C₃ species including inert N₂ gas using C-SR and CL-SR process in a packed bed reactor was conducted at steam to carbon ratio of 3. The activity of Ni based catalyst on Al₂O₃ and CaO/Al₂O₃ support performing the dual action of catalyst and OC on shale gas feedstock was investigated. The aim of the study was to show the feasibility of shale gas as feedstock of steam reforming processes, as well as demonstrating the catalytic, reduction behaviour and cyclic stability of the materials in question (NiO on Al₂O₃ and CaO/Al₂O₃ support) for shale gas CL-SR.

Materials and methodology

Experimental materials

The model shale gas mixture used for the experimental was reproduced from cylinders of different hydrocarbons. Pure CH₄ gas used for the experiments was obtained through the laboratory piping (cylinder of CP grade 99.9%), while a mixture of 50% C₂H₆ and C₃H₈ in an AZ size cylinder (1.2 L water capacity) containing 50% inert N₂ gas (for safety reasons and

ease of elemental balance) was synthesised and obtained from BOC to reproduce a mixture gas feed in the experimental set up of 40.1% C₂H₆, 9.9% C₃H₈ and 50% N₂. The desired molar composition (Table 1) was calculated based on the mole fraction of the species and a given total volumetric flow rate, selected according to desired gas hourly space velocity (GHSV). A nitrogen gas to carbon ratio (N:C) of 9.2 (N₂ obtained through the laboratory piping) was maintained in all the experiments to aid in the calculation of process outputs. The model shale gas presented in Table 1 corresponds to a typical composition of natural gas, containing approximately up to 80% of methane with the balance consisting of the higher hydrocarbons (>C₁), CO₂ and inert N₂ gas [50], representing a mixture richer in ethane and propane than conventional gas. This composition can also be representative of typical composition of natural gases from Nigeria [51] and the North Sea UK [52], by containing up to 80% methane [52]. The gas is an actual shale gas composition from the United States; extracted from a Marcellus shale, which lies in western Pennsylvania, Ohio and West Virginia [53].

Nickel based catalyst on aluminium oxide support (18 wt. % NiO on Al₂O₃ support) and nickel oxide on calcium aluminium oxide support (15 wt. % NiO on CaO/Al₂O₃ support) were provided by Twigg Scientific & Technical Ltd for the experimental study. The characteristics of the materials used as catalyst and/OC are given in Table 3.

Experimental rig description

The experimental rig schematic shown in Fig. 1 is integrated with a down flow quartz reactor (manufactured by York Glass Ltd), with an inner diameter of 12 mm and the length of 495 mm, held inside an electric tube furnace (Elite Thermal Systems Ltd. TSV12/50/300), where insulating mineral wool of about 2–3 mm thickness was placed between the quartz reactor and the furnace's bore. The quartz reactor was used in a packed bed configuration, i.e. it housed the steam reforming catalyst doubling as OC as a fixed bed of particles. The temperature of the reactor was monitored in real time online using Picolog software by K-type thermocouple as shown in the schematic. A programmable syringe pump (New Era pump system) controlled the flow rate of water to the reactor. The syringe pump was connected to the reactor through an injector system. The gas flows of H₂ (used for reduction of the catalyst), N₂ (inert gas), air (oxidant in chemical looping runs), and fuel feed (shale gas C₂/C₃/N₂ mixture, and CH₄) were controlled by four separate MKS mass flow controllers. The latter regulate flow rates according to given set points via the control valves. A coolant (mix of ethylene glycol and water in the volume of 1:1) at –6 °C was circulated between the

Table 1 – Composition and molar flow rate of shale gas used for experiments.

Species	Composition (%) [53]	Molar Flow (mol/s)
CH ₄	79.4	2.68 × 10 ⁻⁶
C ₂ H ₆	16.1	5.44 × 10 ⁻⁷
C ₃ H ₈	4.0	1.35 × 10 ⁻⁷
N ₂	0.4	1.35 × 10 ⁻⁸
Total	100	3.37 × 10 ⁻⁶

Table 2 – Comparison of CL-SR with C-SR process and equilibrium results H₂ yield and purity, fuel and water conversion at 1 bar, GHSV 0.498, S:C 3 (average values). Reforming/reduction reaction at 750 °C and oxidation reaction at 750 °C with 15 wt. % NiO on CaO/Al₂O₃ support as catalyst/OC.

Number of cycle	H ₂ yield (wt. % of fuel)	H ₂ purity (%)	Fuel conversion (%)	H ₂ O conversion (%)
1st	31.593	71.318	81.684	33.489
2nd	29.535	69.788	78.398	30.375
3rd	33.239	71.713	82.518	37.176
4th	36.708	73.794	86.778	43.278
5th	37.804	74.484	87.619	45.544
6th	36.727	73.840	87.044	43.151
7th	37.826	74.308	88.274	45.163
8th	37.152	74.033	84.892	45.680
9th	26.019	68.372	72.153	25.473
10th	24.417	67.281	69.445	23.149
11th	26.187	67.828	70.050	27.309
12th	26.595	68.306	72.328	26.842
13th	26.606	68.253	72.084	27.031
14th	26.477	67.842	71.301	27.222
15th	26.479	67.991	71.217	27.284
16th	27.674	69.063	74.817	27.963
17th	26.928	69.036	75.087	25.861
18th	26.741	68.465	73.706	26.300
19th	26.696	68.033	73.553	26.286
20th	26.595	68.306	72.328	26.842
C-SR results				
N/A	31.593	71.318	81.684	33.489
Equilibrium results				
N/A	41.27	76.16	99.90	49.02

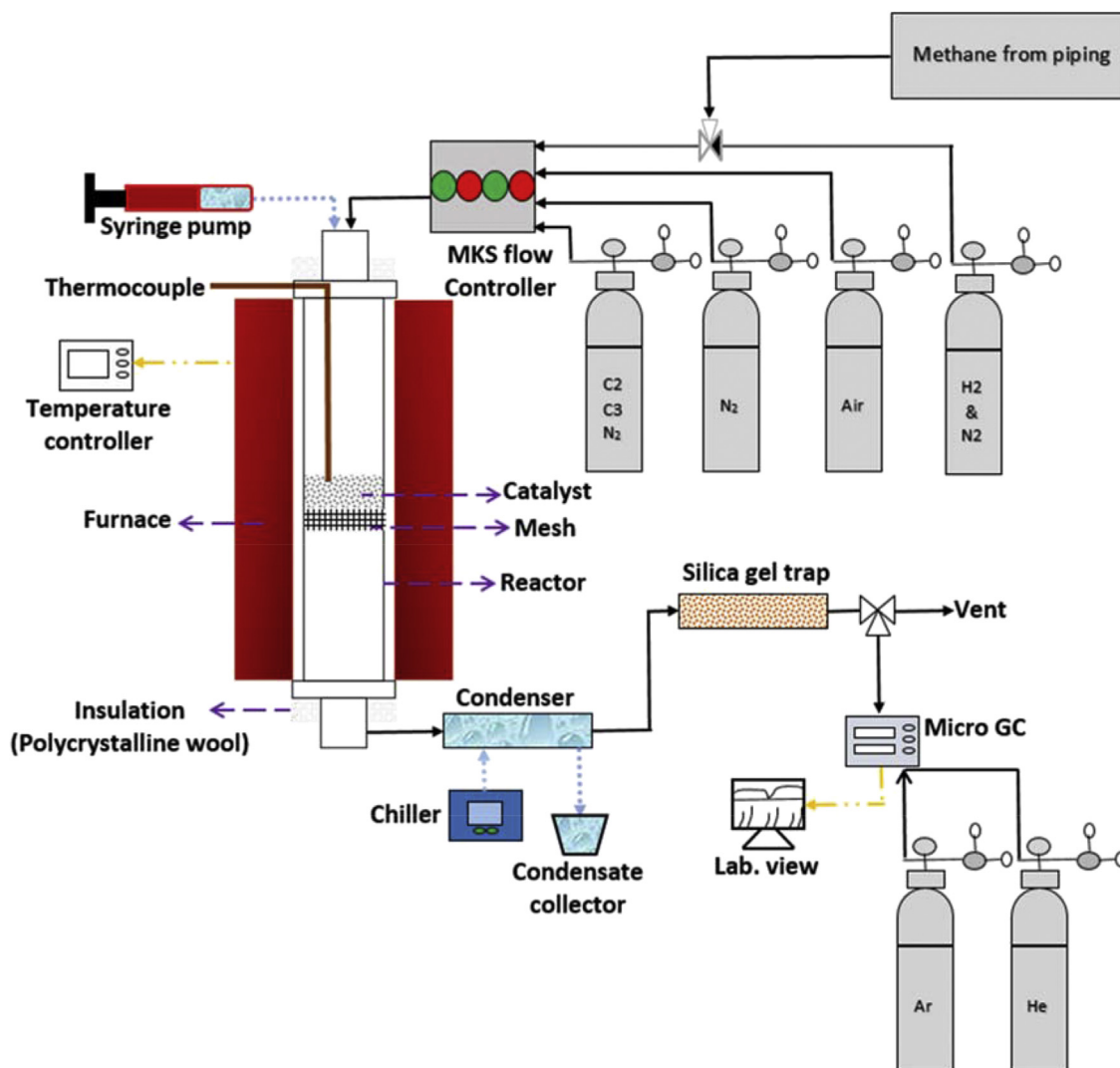
condenser and a chiller (Fisher Scientific 3016S) to maintain the condenser at a low temperature (–6 °C). The condenser cooled the hot product gases leaving the reactor and moisture was trapped by silica gel before going to the micro-gas chromatograph (micro GC) for analysis. The presence of nitrogen gas in the feed aided calculation of parameters such as gas products yield and feedstock conversion using elemental balances.

Experimental procedure

All units of experimental rig were thoroughly cleaned with acetone before each experimental run. The catalyst was crushed using pestle and mortar and sieved to 1.2 mm mean size using 1.4 and 1.00 mm mesh. The particle size of the catalyst was chosen in the knowledge that diffusion as well as kinetic rate limitation were likely, as would be expected of a larger scale set up but that pressure drop would be limited. This was motivated by simulating conditions close to those used in the steam reforming industrial plants, and not with the aim of deriving kinetics which would have required much smaller particle size. 3 g of catalyst was loaded into the reactor (random packing) before setting up the experimental rig as shown in the schematic. The furnace was set to the desired experiment temperature e.g. 600 °C. Each C-SR experiment consisted of 2 major stages; reduction of catalyst and steam reforming process. In the first cycle of CL-SR, and in C-SR, reduction of the catalyst from NiO to active Ni was preceded using 5 vol % hydrogen in nitrogen carrier gas. The nitrogen

Table 3 – CL-SR process characterization results at 1 bar, GHSV 0.498 and S:C 3. For CL-SR Reforming/reduction reaction at 750 °C and oxidation reaction at 750 °C. Reacted catalyst/OC after the last (20th) oxidation cycle (Table 1 inputs).

Condition	NiO/Ni crystallite size (nm)	BET Surface area (m ² /g)	C (wt. %) on catalyst	C (mol) on catalyst	C (g/L) in condensate
C-SR process results					
Reduced with H ₂ Ni/CaO/Al ₂ O ₃	18.15	36.751	N/A	N/A	N/A
750 °C with Ni/CaO/Al ₂ O ₃	18.43	16.175	0.40	0.0010	0.040
CL-SR process results					
Fresh NiO/CaO/Al ₂ O ₃ catalyst/OC	20.00	21.31	N/A	N/A	N/A
Reacted at 750 °C (NiO/CaO/Al ₂ O ₃ catalyst/OC)	19.00	23.82	7.59	0.0205	0.069

**Fig. 1 – Schematic diagram of experimental rig.**

and hydrogen flow rate were 200 and 10 cm³ min⁻¹ (STP) respectively. Reduction resulted in micro GC H₂ vol% reading which remained at zero, and then returned to 5 vol % after about 45 min approximately, indicating that the catalyst had completed its reduction step. Hydrogen flow was then stopped leaving only the nitrogen feed until the hydrogen reading reached 0% again, having flushed out all the reducing H₂ in the reactor. This was followed by the steam reforming process,

which started by feeding water and fuel (shale gas) to the reactor using the programmable syringe and MKS flow controllers respectively. Steam and fuel were fed into the reactor at the desired molar steam to carbon ratio. Experiments lasted for at least 1–2 h and ended by turning off the water and fuel flows first, then the furnace, thus leaving only nitrogen flow to completely flush the reformat gases out and aid in cooling down the reactor. Once the furnace temperature dropped

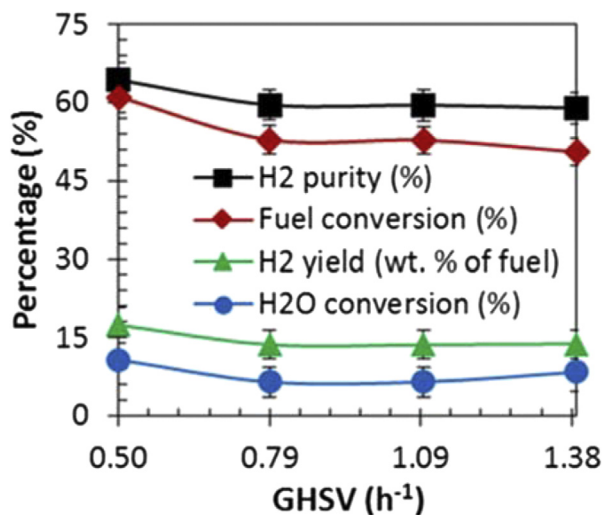


Fig. 2 – Effect of GHSV on H₂ yield and purity, fuel and H₂O conversion using 18 wt. % NiO on Al₂O₃ support at 1 bar, 650 °C and S:C 3 (average values).

down to 25 °C, the chiller was turned off and the rig was ready to be dismantled and set for the next experiment. Experimental results were collected online from a laboratory computer.

For chemical looping steam reforming experiments, the oxidation reaction (using air feed) marked the end of each cycle. Cycle 1 began from a H₂ reduced catalyst OC, but subsequent cycles followed from an air feed and auto-reduction by the fuel itself took place. Re-oxidising the catalyst also burned off carbon that might be deposited on the catalyst. An air flow of 500 cm³ min⁻¹ STP and 750 °C was used. As mentioned earlier, the oxidation stage marked the end of each cycle. The recorded temperature during air feed was seen to increase by roughly 10–15 °C owing to the oxidation reactions of the carbon residue and re-oxidation of the nickel-based catalyst. The reduction stage lasted 3–5 min, whereas the steam reforming stage lasted a minimum of 1 h in each cycle.

Definition of process outputs

A nitrogen balance was used to facilitate the calculation of the total gas moles produced for the initial mixture chosen ($\dot{n}_{out,dry}$) and derive gas products yields and reactants conversions X_i and selectivity of carbon to either CH₄ or other carbon containing gas species 'S_{C to CH₄ or CO or CO₂ etc.' as shown in Eqs. (1)–(6). Presentation and definition of process outputs was based on the following:}

$$\dot{n}_{out,dry} = \frac{\dot{n}_{N_2,in}}{y_{N_2}} \quad (1)$$

where \dot{n}_{N_2} stands for molar flow rate of nitrogen, y_{N_2} is mole fraction of N₂ obtained from the gas chromatography, and 'in' for initial or input. Thus, the molar rate of any product gas 'i' can be calculated as follows;

$$\dot{n}_i = y_i \times \dot{n}_{out,dry} \quad (2)$$

where 'i' stand for molar flow rate and 'y_i' for mole fraction obtained from the gas chromatography. A carbon balance was used to calculate the fuel conversion X_{gas} to the main carbon containing products according to the following equation;

$$X_{gas}(\%) = \frac{T_{nC,in} - (\dot{n}_{CH_4} + 2\dot{n}_{C_2H_6} + 3\dot{n}_{C_3H_8})_{out}}{T_{nC,in}} \times 100 \quad (3a)$$

$T_{nC,in}$ is the molar rate of total number of initial carbon in the fuel. It can also be written as;

$$X_{gas}(\%) = \frac{(\dot{n}_{CH_4} + 2\dot{n}_{C_2H_6} + 3\dot{n}_{C_3H_8})_{in} - (\dot{n}_{CH_4} + 2\dot{n}_{C_2H_6} + 3\dot{n}_{C_3H_8})_{out}}{(\dot{n}_{CH_4} + 2\dot{n}_{C_2H_6} + 3\dot{n}_{C_3H_8})_{in}} \times 100 \quad (3b)$$

Note that despite monitoring the C₂H₆ and C₃H₈ leaving the reactor by micro-GC, neither were detected during the course of the experiments, leaving CH₄ as the only hydrocarbon product.

H₂ yield was defined as shown in Eq. (4) and H₂ purity was defined using Eq. (5).

$$H_2 \text{ yield (wt. \%)} = \frac{100 \times 2.02 \left(\frac{g \text{ of } H_2}{mol \text{ of } H_2} \right) \times \dot{n}_{H_2}}{MW_{gas} \left(\frac{g \text{ of } gas}{mol \text{ of } gas} \right) \times \dot{n}_{gas \text{ in}}} \quad (4)$$

where \dot{n}_{H_2} stand for molar flow rate of H₂ out, $\dot{n}_{gas \text{ in}}$ molar flow rate of gas in and MW_{gas} stand for molecular weight of gas in grams

$$H_2 \text{ purity (dry basis \%)} = \frac{\dot{n}_{H_2}}{\sum \dot{n}_{all \text{ dry gases, without } N_2}} \times 100 \quad (5)$$

Steam conversion fraction during the fuel/steam/N₂ feed; when steam reforming is coupled with water gas shift, the production of hydrogen is the result of the contributions of the fuel–hydrogen and of the steam–hydrogen. Generally, for a 'C_nH_m' fuel reacting with (2n) H₂O via steam reforming and the water gas shift reactions, the maximum production of H₂ is (2n + 0.5 m), indicating clearly that in conditions of maximum H₂ production, the steam contribution fraction is (2n)/(2n + 0.5 m) and that of the fuel, 0.5 m/(2n + 0.5 m). For the shale gas used for the experimental studies (containing CH₄, C₂H₆, and C₃H₈), the steam contribution can therefore account for 52.6% of the H₂ produced through SR and WGS, while that of the fuel is 47.4%. Thus steam conversions, which are hardly reported in literature, have a great effect on the H₂ yield of the steam reforming process. Factors limiting the steam conversion are not only equilibrium limitations, but also the catalyst's activity in both the steam reforming and the water gas shift reactions. Using hydrogen elemental balance, a minimum value for the steam conversion fraction can be estimated using Eq. (6):

$$X_{H_2O} = \frac{1}{\dot{n}_{H_2O,in}} [(2\dot{n}_{CH_4} + 3\dot{n}_{C_2H_6} + 4\dot{n}_{C_3H_8} + \dot{n}_{H_2}) - 0.5m(\dot{n}_{gas,in} X_{gas})] \quad (6)$$

where m is the moles of atomic H in the fuel. The first, positive term in Eq. (6) represents the formation of the hydrogen containing products and the second negative term accounts for the known contribution of the fuel to the hydrogen products, leaving only the contribution of water to the system.

Characterization

PANalytical X'pert MPD instrument using Cu K α radiation was used to obtain the X-ray diffraction (XRD) patterns of unreacted and reacted catalysts. X'Pert HighScore Plus software was used for phase analysis of the XRD data. Quantification of the XRD data; catalyst/OC (respective amounts of NiO and Al₂O₃ (18 wt. % NiO on 82 wt. % Al₂O₃ support and 15 wt. % NiO on 85 wt. % CaO/Al₂O₃ support)) as well as crystalline size of the materials (Table 3) was calculated using the Rietveld refinement method and the Scherrer equation respectively.

Field-emission scanning electron microscope (FESEM, LEO Gemini 1530) was used to study surface morphology of the unreacted and reacted catalyst/OC. The sample particles were coated with an Iridium layer of 10 nm and used for FESEM imaging. Energy dispersive X-rays (EDX) was used for further analyses such as element identification of the fresh and used/ reacted catalyst/OC.

CHNS Elemental Analyser (Flash EA2000 by CE Instruments) was used to measure the quantity of carbon deposited on the reacted catalyst/OC. The catalyst/OC were ground to fine powder before the CHNS measurements. 8 mg (approximately) of each sample was used for each analysis.

In order to know the actual carbon (total organic and inorganic carbon) generated during experiments, carbon content in the condensate (collected at the bottom of the reactor, see rig schematic in Fig. 1) was measured using a Hach-Lange IL550 analyser.

Chemical equilibrium calculations

Minimisation of Gibbs free energy was used to conduct the chemical equilibrium studies. The GEA (Chemical Equilibrium and Applications) software by NASA [54] was used to perform the thermodynamic equilibrium calculations. All the gaseous reactants (CH₄, C₂H₆, C₃H₈, N₂, CO₂ and H₂O) and potential products (H₂, CO, C_(s), and NH₃ etc.) were considered at equilibrium. Other related species such as CH₂, CH₃, and CH₂OH etc. were also included in the equilibrium calculations but their molar fractions were less than 5×10^{-6} , therefore considered negligible. A carbon balance was used to facilitate the calculation of the equilibrium total moles produced for the initial mixture chosen and derive products yields and reactants conversions. The authors applied their own post processing procedures allowing the calculations of reactants conversions and molar yields of products, full details of thermodynamic and post processing procedures can be found in Ref. [17].

Results and discussion

Conventional steam reforming (C-SR) of shale gas experiments

Effect of gas hourly space velocity (GHSV) on C-SR process

The effect of gas hourly space velocity (GHSV) was investigated at 1 bar, S:C ratio of 3 and 650 °C using the steam reforming catalyst 18 wt. % NiO on α -Al₂O₃ support as shown

in Fig. 2. GHSV is defined as the total volumetric flow rate of feedstock (gas + steam + N₂) divided by the volume of catalyst. It was found that GHSV significantly affects fuel and water conversion and subsequently H₂ yield and purity as well. As expected, the fuel (shale gas) conversion increases as the GHSV decreases (from 1.393, 1.094, 0.793 to 0.498), while all other parameters are kept constant. Consequently, the lowest GHSV (0.498) with the highest contact time was chosen as the best for the range of conditions investigated and used for all the subsequent experiments. Maximum fuel conversion i.e 100% was not achieved even at the highest contact time (GHSV 0.498 h⁻¹). Comparison of the experimental results with the equilibrium results showed that the experimental results are away from equilibrium which could be attributed to mass transfer and kinetic limitations causing low fuel and water conversion and subsequently low H₂ yield and purity. Table 1 in the supplementary data presents a comparison between the experimental (average values) and equilibrium data. Previous studies on the effect of GHSV on steam reforming process such as Cavallaro et al. [55], Xu et al. [56], Jiwanuruk et al. [57] and Abbas et al. [41] also found that increasing the GHSV resulted in a decrease in fuel conversion, which in turn affected both the H₂ yield and purity negatively depending on the extent of increase.

Effect of catalyst support on C-SR process

The performance of each catalyst (provided by the manufacturer TST LTd as 18 wt. % NiO on α -Al₂O₃ support and 15 wt. % NiO on CaO/Al₂O₃ support) was investigated over a range of temperature (600–750 °C). Both catalysts were reduced with 5% H₂ (balance N₂) at 700 °C for an hour to convert the NiO to active Ni. No significant difference was found between the two catalyst at low/medium temperature range (600 and 650 °C). However, at higher temperature (700 and 750 °C), the Ni on CaO/Al₂O₃ support performed better/was more active than the Ni on Al₂O₃ support with regards to product yield and feed conversion as depicted in Fig. 3. 36% rise in H₂ yield and 8% rise in H₂ purity was seen between the two catalyst average outputs at 750 °C under same operating condition (1 bar, S:C 3 and GHSV 0.498).

This was expected because the presence of CaO in the catalyst will decrease its acidity (from Al₂O₃ support) [58], consequently decreasing the chances of solid carbon deposition on the catalyst that tends to occur at higher temperatures. Thus, effectively increasing the feed conversion (fuel and H₂O conversion), which in turn positively enhance the H₂ yield and purity. Previous studies by Basagiannis and Verykios [58] on steam reforming of acetic acid has proved that the acidity of alumina support favours solid carbon decomposition in a significant amount. Van Beurden [59] also reported acidic support enhance cracking of CH₄, therefore generating carbon. As a result, feed conversion and product yield are affected negatively to a large extent.

Effect of temperature on C-SR process

C-SR process experiments were conducted isothermally using shale gas as feedstock (see Table 1 for composition) in a packed/fixed bed reactor at atmospheric pressure. The effect of temperature was investigated at 1 bar, S:C ratio of 3 and the temperature range of 600–750 °C. The choice of S:C ratio of 3

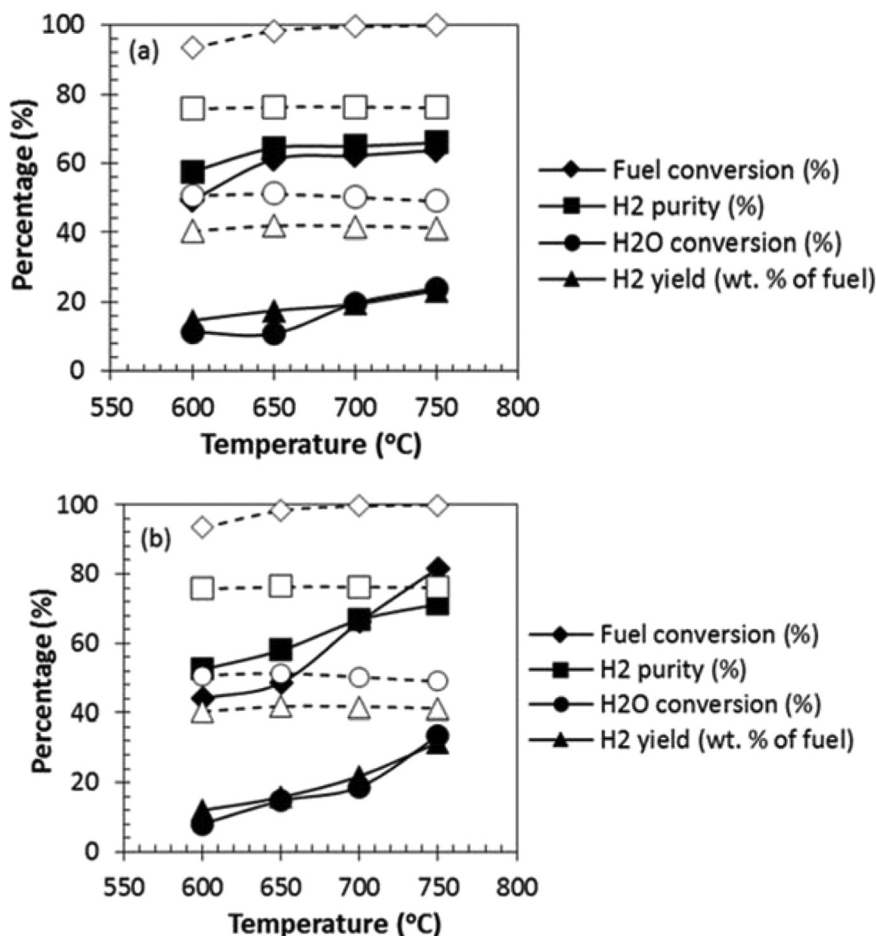


Fig. 3 – Comparative analysis between experimental (average) process output and chemical equilibrium results at 1 bar, GHSV 0.498 and S:C 3 (a) using 18 wt. % NiO on Al₂O₃ support catalyst (b) using 15 wt. % NiO on CaO/Al₂O₃ support catalyst (Note: Solid lines are for experimental results and dashed lines for chemical equilibrium results).

was due to the fact that is the condition of excess steam typically used in industrial steam methane reforming, aimed at H₂ production rather than syngas generation. The condition was also found to be optimum from our previous thermodynamic studies [17].

Fuel and H₂O conversion, H₂ yield and purity increased as temperature increased. This was because high temperatures are in favour of the strong endothermic steam reforming reaction in accordance with Le Chatelier's principle (Fig. 3). As the temperature of the reforming process increases, CH₄ outlet moles decreases indicating increase in fuel conversion consequently increasing the outlet moles of H₂. The C₂H₆ and C₃H₈ species in the fuel were completely reformed to syngas and/or cracked to CH₄ as confirmed by the continued absence of these species in the outlet product gases. The endothermic steam reforming of CH₄ was enhanced by an increased temperature to the detriment of methanation reaction that is favoured in the low/medium temperature range.

Comparison of the experimental results with the thermodynamic equilibrium results show the same trend with respect to temperature. However, the experimental process outputs were far from the thermodynamic equilibrium results. Thus, the chemical equilibrium results demonstrated

higher fuel and water conversion and consequently higher H₂ yield and purity. Reaction kinetics (reaction rate of methane on a conventional nickel on alumina support depend on the partial pressure of methane [59]) and thermodynamic equilibrium limitation (depicted in Fig. 3) can explain the findings. It can be concluded that water gas shift reaction (WGS) was poorly active in all the temperature range investigated (during the experimental studies) particularly at 700 and 750 °C owing to the medium/high concentration of CO outlet moles (Fig. 4) depending on the temperature. Again, the outlet moles of the chemical equilibrium results showed exactly same trend as the experimental results except that the WGS reaction was more active in the chemical equilibrium system compared to the experiments.

The inhibition of the exothermic WGS reaction no doubt could be attributed to the unfavourably high temperature. However, at 600 and 650 °C (with 15 wt. % NiO on CaO/Al₂O₃ support) the outlet moles of CO₂ were higher than those of CO (see Fig. 4 (b) for clarity), this results from the fact that the low/medium temperature range favours the reaction even though it is not the optimum/desirable temperature for the WGS reaction. The contribution of CH₄ (from the feedstock and that from the cracking of C₂-C₃ species) steam reforming to

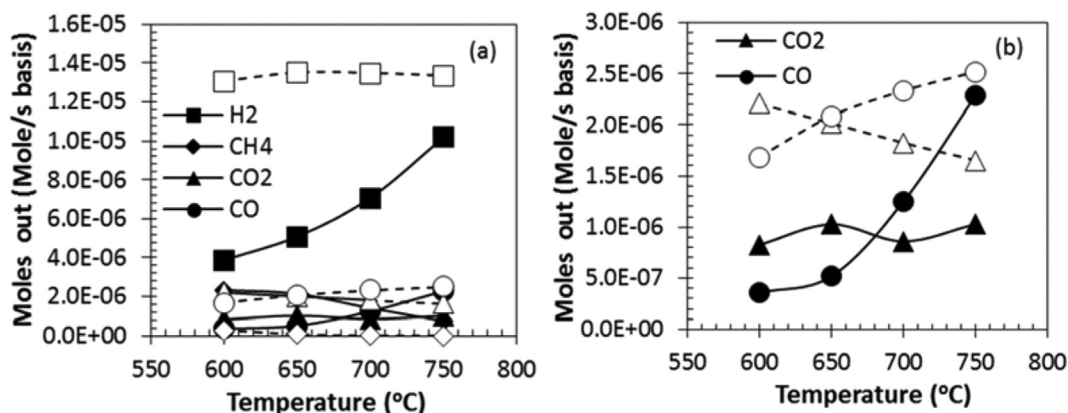


Fig. 4 – Comparative analysis between experimental (average) process output and chemical equilibrium results at 1 bar, GHSV 0.498 and S:C 3 using 15 wt. % NiO on CaO/Al₂O₃ support catalyst (a) outlet moles (b) Clearer graph of CO₂ and CO moles out.

generate H₂ compensated the diminution in H₂ production caused by the inhibition of WGS reaction. Generally speaking, the suppression of two exothermic reactions (WGS and Boudouard reactions) by high temperatures causes the increase in the CO concentration and a decrease in the CO₂ concentration as shown in Fig. 4. Fig. 5 shows the plots of process outputs with time on stream at 750 °C. Fuel and H₂O conversion, H₂ yield and purity are fairly stable over the duration of (all) the experiments. Molar production rate of H₂, CH₄ and CO were also stable.

H₂ production using methane and natural gas steam reforming in a conventional and microreactor reaction systems was investigated by Izquierdo et al. [60] with Ni based catalyst supported on MgO and Al₂O₃ and Pd and Pt based catalyst supported on Al₂O₃. They investigated the influence of temperature and S:C ratio, at atmospheric pressure and constant GHSV, on the catalytic activity and concluded that increasing the temperature improved fuel conversion but did not improve considerably at higher S:C ratios. The influences of temperature on C-SR reported is in good agreement with

those of the present study. Abbas et al. [41] conducted a kinetics study and modelling of steam methane reforming process over a NiO/Al₂O₃ catalyst in an adiabatic packed bed reactor. They found that higher temperature had a positive effect on H₂ yield and purity and concluded that high temperature, low pressure and high steam to carbon ratio are the optimal operating conditions with regards to fuel conversion and H₂ purity, which are in good agreement with the present study and equilibrium predictions.

Chemical looping steam reforming (CL-SR) process of shale gas

Effect of chemical looping on steam reforming process

Reduction-oxidation multicycles were conducted in a fixed bed reactor with NiO based oxygen carrier (OC) performing the dual action of both the OC and reforming catalyst. 3 g of the OC/catalyst was placed in the quartz reactor.

The CL-SR process experiments were conducted at 1 bar, S:C 3 and GHSV of 0.498 at 750 °C (with NiO on CaO/Al₂O₃

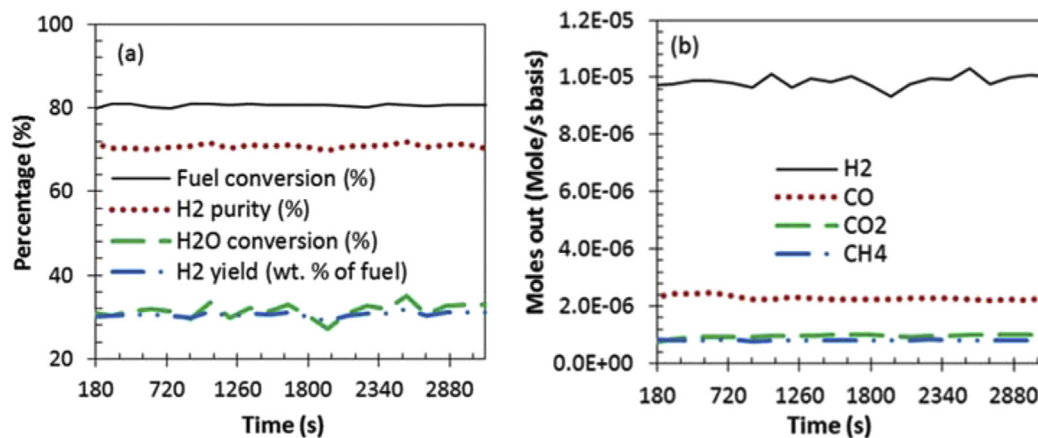


Fig. 5 – Process output vs time at 750 °C, 1 bar, GHSV 0.498 and S:C 3 using 15 wt. % NiO on CaO/Al₂O₃ support catalyst (a) H₂ yield and purity, fuel and H₂O conversion vs time (b) moles produced vs time.

support). 20 reduction-oxidation cycles were performed for the investigated temperature/catalyst/OC. Simultaneous reforming and reduction of catalysts/OC with the fuel was possible at the reaction temperature, as further confirmed by good selectivity towards the desired products (H_2 and CO_2). This shows that the use of shale gas or gas with higher composition of C2 and C3 species as a feedstock for the CL-SR process is feasible.

The molar production rate of H_2 was higher than that of the other gaseous products CO , CO_2 , and CH_4 as depicted in Fig. 6. The molar production rates of CO and CO_2 were fairly stable (from the first to the 8th where a sudden decrease was observed in the 9th cycle that fairly stabilizes too to the last cycle.) and dependent on the fuel and water conversion rate. The latter is because steam is a reactant in the WGS reaction that produces CO_2 . The molar output rate of CH_4 was lower than those of CO and CO_2 in the first 8 cycles. However, the output rate increased gradually from the 9th cycle, stabilizing and merging with the production rate of CO at approximately the 11th to the last cycle (20th). In Fig. 6 after the 8th cycle the production rate of CO was constant due to less active WGS reaction causing the decrease of CO_2 output. On the other hand, the production rate of CH_4 was high no doubt due to low fuel conversion. The observe phenomenon in general could result from the fact that the activity of the catalyst/OC was decreasing with increasing number of cycles. As further confirmed by the decrease in fuel conversion in the cycles. Solid carbon deposition on the surface of the catalyst/OC might also be the reason of the low activity and subsequently low fuel conversion [61].

Fuel and water conversion, H_2 yield and purity increased in the CL-SR process as shown in Table 2 (prior to the catalyst/OC deactivation) compared to the C-SR process; even though part of the fuel was used for the reduction process (co products CO and H_2 or CO_2 and H_2O). Table 2 in the supplementary data presents the percentage enhancement of CL-SR process with C-SR process at $750\text{ }^\circ\text{C}$.

The process outputs (yield, purity and conversion for the first 8 cycles and then from 9th to the 20th cycle) were moderately stable with a negligible variation depending on the fuel and water conversion (high or low) as presented in Table 2. Feedstock and water conversion, H_2 yield and purity increased gradually with increase in number of cycles to the

9th cycle, where a gentle dwindling with the cycles was seen that became steady at approximately the 11th cycle to the end. Surprisingly, the decrease in the process outputs was lower than the C-SR process. The decrease in process outputs might have resulted from the activity of the catalyst/OC decreasing with time, solid carbon formation on the surface of the catalyst/OC and Ni active site blockage. The gradual increase in H_2 yield and purity and fuel and water conversion after the 2nd cycle might not only be attributed to the initial good performance of the catalyst/OC but also to the fact that Ni activity increases after first contact with fuel [26]. The first cycle process outputs were exactly the same as the C-SR process further validating the reproducibility of the condition. The sudden drop at the 9th cycle rather than in a gradual decreasing mode could be attributed to a number of factors as well such as sudden drop in the activity of the catalyst/OC, carbon deposit accumulation over the period of the first 8 cycles or even sudden blockage of Ni active site.

Oxidation of the catalyst/OC at $750\text{ }^\circ\text{C}$ to return it back to its original form (NiO) as well as to burn off any carbon deposits on the surface of the catalyst/OC with air depict an increase in the oxidation temperature ($10\text{--}15\text{ }^\circ\text{C}$ roughly) as expected owing to the exothermicity of the reaction. The burning off of the solid carbon (coke) deposition during the air feed was coincidental with CO_2 and CO generation. Full details and discussion of the reduction and oxidation reaction process are not available owing to the fact that the micro GC takes readings every 3 min, thus the most significant part of these rapid processes were missed.

The experimental results were found to be away from the chemical equilibrium results as depicted in Table 2. Catalyst selectivity [62], reaction kinetics and mass transfer limitation might contribute to the observed phenomenon.

It is difficult to compare the results of the present studies with previous research work directly because most of the studies in CL-SR used low steam to carbon ratios [44–46,63] or focused on pure methane as a feedstock [40]. Antzara et al. [40] investigated the performance of NiO based catalyst/OC supported on ZrO_2 , TiO_2 , SiO_2 , Al_2O_3 and $NiAl_2O_4$ for CL-SR of CH_4 . Conditions for twenty reduction cycles in a fixed bed flow unit at $650\text{ }^\circ\text{C}$, S:C 3, GHSV 100,000. They found that NiO/Al_2O_3 support demonstrated a high initial activity, but also high deactivation, leading to methane conversion of 59% at the end

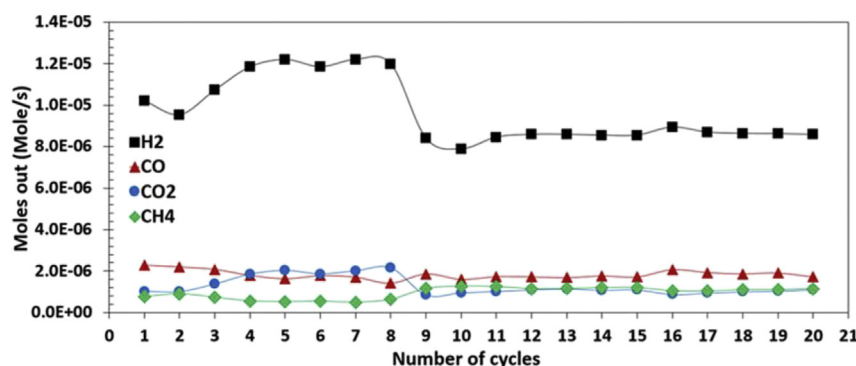


Fig. 6 – Moles out at 1 bar, GHSV 0.498 and S:C 3 (average values). Reforming/reduction reaction at $750\text{ }^\circ\text{C}$ and oxidation reaction at $750\text{ }^\circ\text{C}$ with 15 wt. % NiO on CaO/Al_2O_3 support as catalyst/OC.

of the test. The high initial activity of catalyst/OC (NiO/Al₂O₃ support) and high deactivation towards the end of the test is in good agreement to those reported in the present study.

Cyclic stability of output during CL-SR process

To investigate the OC stability/lifetime, 20 reduction cycles were conducted at 750 °C using NiO on CaO/Al₂O₃ support as catalyst/OC. Table 2 depicts the process outputs of 20 reduction cycles. Even though the sudden decrease in the activity of the catalyst/OC could be attributed to the high temperature used that promotes solid carbon deposition, the sudden drop of the activity of the catalyst/OC at the 9th cycle is seen as too early. This is because the air feed step (oxidation of the Ni to NiO) is accompanied by burning off of the solid carbon deposit

on the surface of the catalyst/OC. Nonetheless, the observed phenomenon could be attributed to significant coke deposition accumulated over the range of the cycles [64,65] or even extensive sintering of the Ni particles on the surface of the catalyst/OC [40,66]. To evaluate the mentioned possibilities, characterization of the catalyst/OC before and after the 20 reduction-oxidation cycles was performed and discussed in the next section.

Fig. 7 (a and b) shows the plots of process outputs with time on stream of the 8th cycle at 750 °C using 15 wt. % NiO on CaO/Al₂O₃ support catalyst/OC. Fuel and H₂O conversion and H₂ yield and purity were stable over the duration of the experiments. Molar production rate of H₂, CH₄ and CO were also stable with insignificant differences over time.

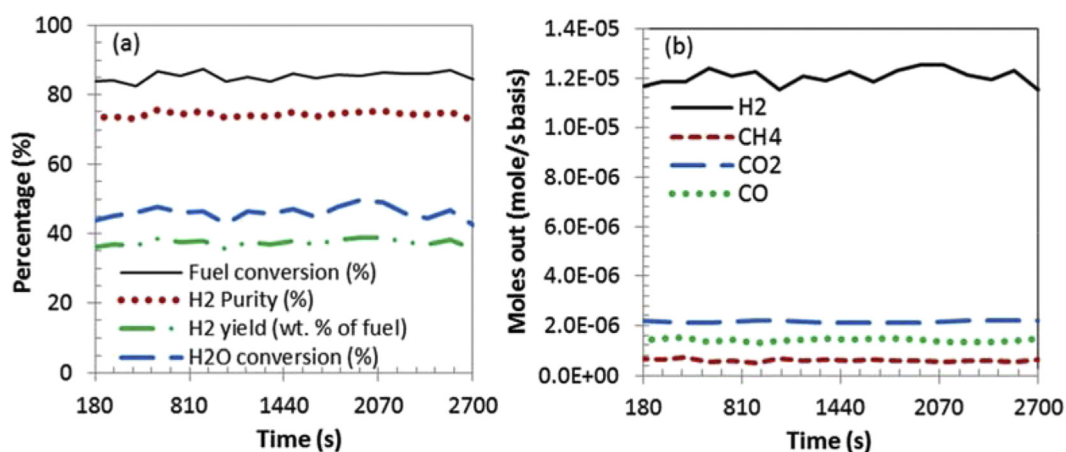


Fig. 7 – 8th cycle process output vs time 1 bar, GHSV 0.498 and S:C 3 using 15 wt. % NiO on CaO/Al₂O₃ support as catalyst/OC. Reforming/reduction reaction at 750 °C and oxidation reaction at 750 °C (a) H₂ yield and purity, fuel and H₂O conversion vs time (b) moles out vs time.

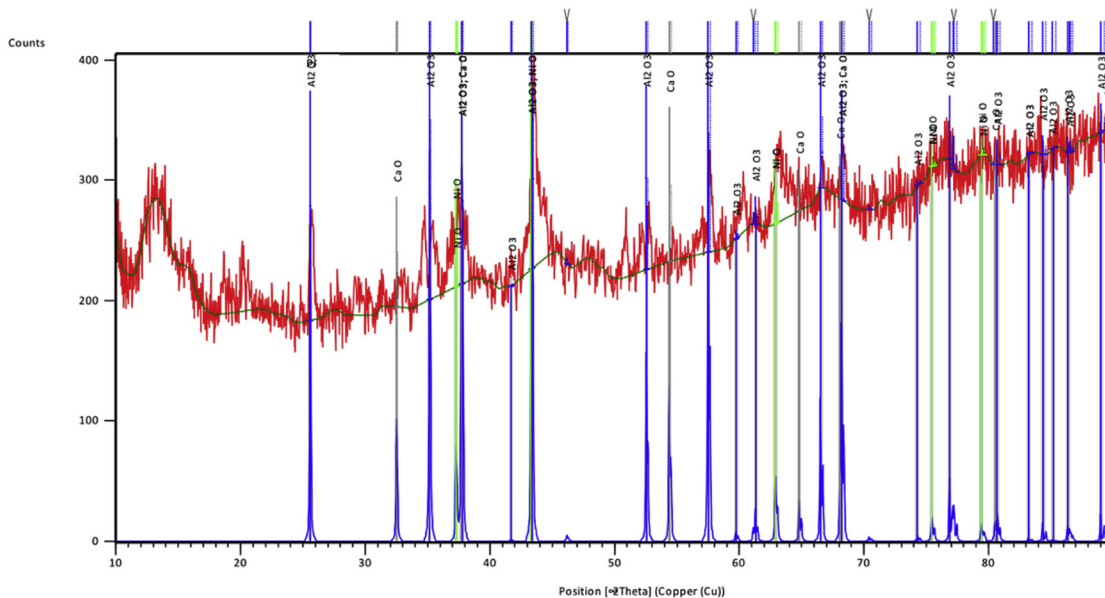


Fig. 8 – XRD diffractogram of fresh 15 wt. % NiO on CaO/Al₂O₃.

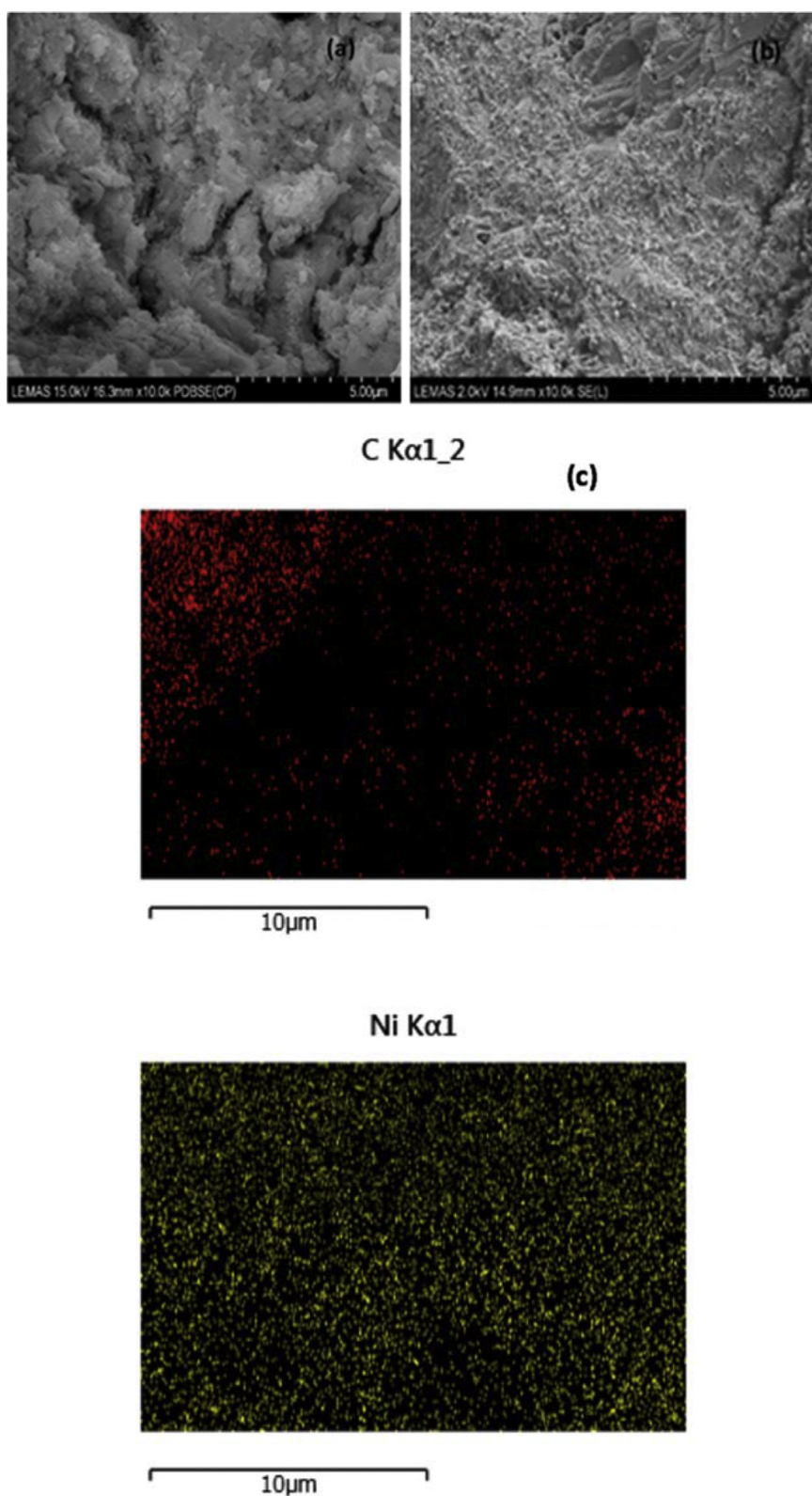


Fig. 9 – FESEM images (a) Fresh 15 wt. % NiO on CaO/Al₂O₃ support catalyst/OC (b) Reacted 15 wt. % NiO on CaO/Al₂O₃ support catalyst/OC at 750 °C 20 cycles (c) EDX Mapping of reacted 15 wt. % NiO on CaO/Al₂O₃ support catalyst/OC at 750 °C after 20 cycles.

Catalyst/Oxygen carrier (OC) characterization

XRD analysis was performed on NiO/CaO/Al₂O₃ but crystallinity degree of the sample is low due to large amorphous content as shown in Fig. 8. However, the average NiO crystallite sizes of the fresh sample and oxidised sample after the 20th cycle (calculated via the Scherrer equation) were in the range of 18–20 nm. The influence on NiO crystallite size after experiments was not evident. The Rietveld refinement method indicated carbon was present in the oxidised sample (after the 20th cycle) in addition to NiO, CaO and Al₂O₃. A slight negligible increase in the BET surface area of the NiO/CaO/Al₂O₃ catalyst/OC was observed after the last (20th) oxidation cycle, but this effect on the catalyst/OC was not evident.

Solid carbon deposition on the surface of the Ni on CaO/Al₂O₃ support catalyst/OC was found to be of just 0.0205 mol, analyzed thrice with CHNS analyser for precision and credibility. Thus, it can be concluded that, the oxidation reaction process did successfully burn off the solid carbon deposit on the surface of the Ni on CaO/Al₂O₃ support catalyst/OC at 750 °C. The TOC analysis in both processes (C-SR and CL-SR) showed zero/no significant amount of carbon in the condensate sample (See Table 3).

Both fresh and used/reacted catalyst (and/or OC in the CL-SR system) were again studied using FESEM. The images of reacted catalyst/OC (Fig. 9 (a and b) (note: figure not shown for C-SR)) were analysed using EDX (mapping method Fig. 9 (c)) it was found that carbon deposits were not uniformly distributed on the surface of the catalyst/OC in both processes. Some parts of the catalyst surface had zero or were nearly free of carbon deposits.

Conclusion

As expected from the bench scale experiments which indicated non equilibrium fuel and steam conversions, increasing the GHSV decreased the contact time of the reactant in the reactor, thus operating at the lowest possible GHSV was more suitable in a steam reforming experiments to achieve higher fuel conversions. High operating temperatures are in favour of the strong endothermic steam reforming reaction but to the detriment of the water gas shift reaction. The influence of catalyst support and NiO loading was not evident at low/medium operating temperature (600 and 650 °C). However, at higher temperature (700 and 750 °C), Ni on CaO/Al₂O₃ support catalyst showed better performance than the Ni on Al₂O₃ support with regards to fuel conversion and product yield caused by the alkalinity of CaO, intended to suppress irreversible solid carbon formation on the surface of the catalyst.

CL-SR of shale gas was conducted at S:C of 3 and GHSV of 0.498. The influence of chemical looping on steam reforming (CL-SR process) was investigated at 750 °C using Ni on CaO/Al₂O₃ support as catalyst/OC. The material demonstrated good performance as catalyst/OC with better process outputs compared to the C-SR process prior to catalyst/OC deactivation. However, a single stepwise deterioration was seen after about 9 successive reduction-oxidation cycles approximately, corresponding to 60 h of testing as well. Nonetheless, fuel conversion was high (over 80% approximately prior to the deterioration of

the catalyst/OC), that can be strongly attributed to the high temperature in favour of steam reforming process. The activity loss of the catalyst/OC might have been caused by selective Ni active site blockage, or even carbon deposition on the catalyst/OC surface or sintering of metal Ni phase.

Acknowledgments

The Petroleum Technology Development Fund (Nigeria) is gratefully acknowledged for the scholarship of Zainab Ibrahim S G Adiya, and we also thank the UKCCSRC EPSRC consortium (EP/K000446/1) for call 2 grant 'Novel Materials and Reforming Process Route for the Production of Ready-Separated CO₂/N₂/H₂ from Natural Gas Feedstocks'. Martyn V. Twigg at TST Ltd is also gratefully acknowledged for providing the catalysts. Data associated with this publication are available from the Research Data Leeds Repository under a CC-BY license at <http://doi.org/10.5518/327>.

Appendix A. Supplementary data

Supplementary data related to this article can be found at <https://doi.org/10.1016/j.ijhydene.2018.02.083>.

REFERENCES

- [1] Momirlan M, Veziroglu T. Recent directions of world hydrogen production. *Renew Sustain Energy Rev* 1999;3:219–31.
- [2] Antzara A, Heracleous E, Bukur DB, Lemonidou AA. Thermodynamic analysis of hydrogen production via chemical looping steam methane reforming coupled with in situ CO₂ capture. *Int J Greenh Gas Control* 2015;32:115–28.
- [3] Adiya ZI SG, Dupont V, Mahmud T. Effect of hydrocarbon fractions, N₂ and CO₂ in feed gas on hydrogen production using sorption enhanced steam reforming: thermodynamic analysis. *Int J Hydrog Energy* 2017;42:21704–18.
- [4] Zhu J, Zhang D, King KD. Reforming of CH₄ by partial oxidation: thermodynamic and kinetic analyses. *Fuel* 2001;80:899–905.
- [5] Rosen MA. Thermodynamic investigation of hydrogen production by steam-methane reforming. *Int J Hydrog Energy* 1991;16:207–17.
- [6] Pasel J, Samsun RC, Tschauder A, Peters R, Stolten D. A novel reactor type for autothermal reforming of diesel fuel and kerosene. *Appl Energy* 2015;150:176–84.
- [7] Adris AM, Pruden BB, Lim CJ, Grace JR. On the reported attempts to radically improve the performance of the steam methane reforming reactor. *Can J Chem Eng* 1996;74:177–86.
- [8] Fernández JR, Abanades JC, Murillo R, Grasa G. Conceptual design of a hydrogen production process from natural gas with CO₂ capture using a Ca–Cu chemical loop. *Int J Greenh Gas Control* 2012;6:126–41.
- [9] Boyano A, Blanco-Marigorta A-M, Morosuk T, Tsatsaronis G. Steam methane reforming system for hydrogen production: advanced exergetic analysis. *Int J Thermodyn* 2012;15:1–9.
- [10] Pérez-Moreno L, Soler J, Herguido J, Menéndez M. Stable hydrogen production by methane steam reforming in a two zone fluidized bed reactor: experimental assessment. *J Power Sources* 2013;243:233–41.

- [11] Patel N, Baade B, Fong LW, Khurana V. Creating value through refinery hydrogen management. Singapore: Asian Refinery Technology Conference; 2006.
- [12] Lee G, Yu J, Golikeri SV, Klein B. Market conditions encourage refiners to recover by-product gases. *Oil Gas J* 2013;111(10).
- [13] Yildirim Ö, Kiss AA, Hüser N, Leßmann K, Kenig EY. Reactive absorption in chemical process industry: a review on current activities. *Chem Eng J* 2012;213:371–91.
- [14] Adhikari S, Fernando S. Hydrogen membrane separation techniques. *Ind Eng Chem Res* 2006;45:875–81.
- [15] Kumar RV, Lyon RK, Cole JA. Unmixed reforming: a novel autothermal cyclic steam reforming process. US: Springer; 2002.
- [16] Speight JG. The chemistry and technology of petroleum Fifth ed. Boca Raton: Taylor and Francis Group, LLC; 2007.
- [17] Adiya ZI SG, Dupont V, Mahmud T. Chemical equilibrium analysis of hydrogen production from shale gas using sorption enhanced chemical looping steam reforming. *Fuel Process Technol* 2017;159:128–44.
- [18] Steinfeld A, Kuhn P, Karni J. High-temperature solar thermochemistry: production of iron and synthesis gas by Fe_3O_4 -reduction with methane. *Energy* 1993;18:239–49.
- [19] Solunke RD, Vesper Gt. Hydrogen production via chemical looping steam reforming in a periodically operated fixed-bed reactor. *Ind Eng Chem Res* 2010;49:11037–44.
- [20] Storset SO, Brunsvold A, Jordal K, Langorge O, Anantharaman R, Berstad D, et al. Technology survey and assessment for piloting of CO_2 capture technologies. SINTEF Energy Reserch, Gas Technology; 2013.
- [21] Adanez J, Abad A, Garcia-Labiano F, Gayan P, Diego LF. Progress in chemical-looping combustion and reforming technologies. *Prog Energy Combust Sci* 2012;38:215–82.
- [22] Dou B, Zhang H, Cui G, Wang Z, Jiang B, Wang K, et al. Hydrogen production by sorption-enhanced chemical looping steam reforming of ethanol in an alternating fixed-bed reactor: sorbent to catalyst ratio dependencies. *Energy Convers Manag* 2018;155:243–52.
- [23] Lua C, Li K, Wanga H, Zhu X, Wei Y, Zheng M, et al. Chemical looping reforming of methane using magnetite as oxygen carrier: structure evolution and reduction kinetics. *Appl Energy* 2018;211:1–14.
- [24] Luo M, Yi Y, Wang S, Wang Z, Du M, Pan J, et al. Review of hydrogen production using chemical-looping technology. *Renew Sustain Energy Rev* 2018;81:3186–214.
- [25] Spallina V, Marinello B, Gallucci F, Romano MC, Van Sint Annaland M. Chemical looping reforming in packed-bed reactors: modelling, experimental validation and large-scale reactor design. *Fuel Process Technol* 2017;156:156–70.
- [26] Ryden M, Ramos P. H_2 production with CO_2 capture by sorption enhanced chemical-looping reforming using NiO as oxygen carrier and CaO as CO_2 sorbent. *Fuel Process Technol* 2012;96:27–36.
- [27] Czernik S, French R, Feik C, Chornet E. Hydrogen by catalytic steam reforming of liquid byproducts from biomass thermoconversion processes. *Ind Eng Chem Res* 2002;41:4209–15.
- [28] Chiron F-X, Patience GS, Riffart S. Hydrogen production through chemical looping using $\text{NiO}/\text{NiAl}_2\text{O}_4$ as oxygen carrier. *Chem Eng Sci* 2011;66:6324–30.
- [29] Simpson AP, Lutz AE. Exergy analysis of hydrogen production via steam methane reforming. *Int J Hydrog Energy* 2007;32:4811–20.
- [30] Rostrup-Nielsen JR, Sehested J, Nørskov JK. Hydrogen and synthesis gas by steam- and CO_2 reforming. *Adv Catal* 2000;47:65–137.
- [31] Joensen F, Rostrup-Nielsen JR. Conversion of hydrocarbons and alcohols for fuel cells. *J Power Sources* 2002;105:195–201.
- [32] Ding Y, Alpay E. Adsorption-enhanced steam–methane reforming. *Chem Eng Sci* 2000;55:3929–40.
- [33] Nicholls T, Gorst I, Lewis L, Ruddy M. Everything you wanted to know about gas. But were afraid to ask. London: Silverstone communications Ltd (Energy Future); 2012.
- [34] Anderson DM, Kottke PA, Fedorov AG. Thermodynamic analysis of hydrogen production via sorption-enhanced steam methane reforming in a new class of variable volume batch-membrane reactor. *Int J Hydrog Energy* 2014;39:17985–97.
- [35] Kargbo DM, Wilhelm RG, Campbell DJ. Natural gas plays in the Marcellus shale: challenges and potential opportunities. *Environ Sci Technol* 2010;15:5679–84.
- [36] Paltsev S, Jacoby HD, Reilly JM, Ejaz QJ, Morris J, O'Sullivan F, et al. The future of U.S. natural gas production, use, and trade. *Energy Policy* 2011;39:5309–21.
- [37] Peng SL. Banking on U.S. shale gas boom, Asia petrochemical firms switch to LPG. Singapore. 2014. <http://www.reuters.com/article/2014/08/21/us-asia-lpg-idUSKBN0GL2AD20140821>. [Accessed 1 October 2014].
- [38] Ortiz M, Gayán P, de Diego LF, García-Labiano F, Abad A, Pans MA, et al. Hydrogen production with CO_2 capture by coupling steam reforming of methane and chemical-looping combustion: use of an iron-based waste product as oxygen carrier burning a PSA tail gas. *J Power Sources* 2011;196:4370–81.
- [39] Silvester L, Antzara A, Boskovic G, Heracleous E, Lemonidou AA, Bukur DB. NiO supported on Al_2O_3 and ZrO_2 oxygen carriers for chemical looping steam methane reforming. *Int J Hydrog Energy* 2015;40:7490–501.
- [40] Antzara A, Heracleous E, Silvester L, Bukur DB, Lemonidou AA. Activity study of NiO -based oxygen carriers in chemical looping steam methane reforming. *Catal Today* 2016;272:32–41.
- [41] Abbas SZ, Dupont V, Mahmud T. Kinetics study and modelling of steam methane reforming process over a $\text{NiO}/\text{Al}_2\text{O}_3$ catalyst in an adiabatic packed bed reactor. *Int J Hydrog Energy* 2016;42:2889–903.
- [42] Nieva MA, Villaverde MM, Monzón A, Garetto TF, Marchi AJ. Steam-methane reforming at low temperature on nickel-based catalysts. *Chem Eng J* 2014;235:158–66.
- [43] Sadooghi P, Rauch R. Experimental and modeling study of hydrogen production from catalytic steam reforming of methane mixture with hydrogen sulfide. *Int J Hydrog Energy* 2015;40:10418–26.
- [44] Rydén M, Lyngfelt A, Mattisson T. Synthesis gas generation by chemical-looping reforming in a continuously operating laboratory reactor. *Fuel* 2006;85:1631–41.
- [45] de Diego LF, Ortiz M, García-Labiano F, Adánez J, Abad A, Gayán P. Hydrogen production by chemical-looping reforming in a circulating fluidized bed reactor using Ni-based oxygen carriers. *J Power Sources* 2009;192:27–34.
- [46] Gayán P, de Diego LF, García-Labiano F, Adánez J, Abad A, Dueso C. Effect of support on reactivity and selectivity of Ni-based oxygen carriers for chemical-looping combustion. *Fuel* 2008;87:2641–50.
- [47] Hafizi A, Rahimpour MR, Hassanajili S. Hydrogen production via chemical looping steam methane reforming process: effect of cerium and calcium promoters on the performance of $\text{Fe}_2\text{O}_3/\text{Al}_2\text{O}_3$ oxygen carrier. *Appl Energy* 2016;165:685–94.
- [48] Go KS, Son SR, Kim SD, Kang KS, Park CS. Hydrogen production from two-step steam methane reforming in a fluidized bed reactor. *Int J Hydrog Energy* 2009;34:1301–9.
- [49] Ryden M, Lyngfelt A, Mattisson T. Chemical-looping combustion and chemical-looping reforming in a circulating fluidized-bed reactor using Ni based oxygen carriers. *Energy Fuel* 2008;22:2585–97.
- [50] Mokhatab S, Poe WA. Handbook of natural gas transmission and processing. second ed. USA: Gulf Professional Publishing; 2012.

- [51] Sonibare JA, Akeredolu FA. A theoretical prediction of non-methane gaseous emissions from natural gas combustion. *Energy Policy* 2004;32:1653–65.
- [52] Peebles MWH. *Natural gas fundamentals*. London: Shell International Gas Limited; 1992.
- [53] Bullin K, Krouskop P. *Composition variety complicates processing plans for US shale gas*. USA: Bryan Research & Engineering, Inc; 2008.
- [54] McBride BJ, Gordon S. *Computer program for calculation of complex chemical equilibrium compositions and applications II. User's manual and program description*. Cleveland, Ohio: Lewis Research Center; 1996.
- [55] Cavallaro S, Chiodo V, Freni S, Mondello N, Frusteri F. Performance of Rh/Al₂O₃ catalyst in the steam reforming of ethanol: H₂ production for MCFC. *Appl Catal A Gen* 2003;249:119–28.
- [56] Xu J, Chen L, Tan KF, Borgna A, Saeys M. Effect of boron on the stability of Ni catalysts during steam methane reforming. *J Catal* 2009;261:158–65.
- [57] Jiwanuruk T, Putivisutisak S, Ponpesh P, Bumroongsakulsawat P, Tagawa T, Yamada H, et al. Effect of flow arrangement on micro membrane reforming for H₂ production from methane. *Chem Eng J* 2016;293:319–26.
- [58] Basagiannis AC, Verykios XE. Reforming reactions of acetic acid on nickel catalysts over a wide temperature range. *Appl Catal A Gen* 2006;308:182–93.
- [59] Van Beurden P. On the catalytic aspects of steam-methane reforming. Energy Research Centre of the Netherlands (ECN); 2004. Technical Report I-04–003.
- [60] Izquierdo U, Barrio VL, Cambra JF, Requies J, Güemez MB, Arias a PL, et al. Hydrogen production from methane and natural gas steam reforming in conventional and microreactor reaction systems. *Int J Hydrog Energy* 2012;37:7026–33.
- [61] Wang K, Dou B, Jiang B, Zhang Q, Li M, Chen H, et al. Effect of support on hydrogen production from chemical looping steam reforming of ethanol over Ni-based oxygen carriers. *Int J Hydrog Energy* 2016;41:17334–47.
- [62] Xiu G, Li P, Rodrigues AE. Adsorption-enhanced steam-methane reforming with intraparticle-diffusion limitations. *Chem Eng J* 2003;95:83–93.
- [63] Dupont V, Ross AB, Hanley I, Twigg MV. Unmixed steam reforming of methane and sunflower oil: a single-reactor process for -rich gas. *Int J Hydrog Energy* 2007;32:67–79.
- [64] Rostrup-Nielsen J, Trimm DL. Mechanisms of carbon formation on nickel-containing catalysts. *J Catal* 1977;48:155–65.
- [65] Rostrup-Nielsen JR. Activity of nickel catalysts for steam reforming of hydrocarbons. *J Catal* 1973;31:173–99.
- [66] Bartholomew CH. Mechanisms of catalyst deactivation. *Appl Catal A Gen* 2001;212:17–60.